Design of a Compact High Isolation 4-Element Wideband Patch Antenna Array for GNSS Applications

MUHAMMAD AWAIS[1,2]**, ABDULLAH MADNI**[3]**, AND WASIF TANVEER KHAN**[3]**, (Member, IEEE)**

[1]Texas Analog Center of Excellence, The University of Texas at Dallas, Richardson, TX 75080, USA
[2]Department of Electrical and Computer Engineering, The University of Texas at Dallas, Richardson, TX 75080, USA
[3]Syed Babar Ali School of Science and Engineering, Lahore University of Management Sciences, Lahore 54792, Pakistan

Corresponding author: Abdullah Madni (19060037@lums.edu.pk)

ABSTRACT This work presents a compact (125 mm diameter) wideband four-element antenna array with a high isolation level for Global Navigation Satellite System (GNSS) anti-jamming applications. The array consists of four identical right hand circularly polarized (RHCP) single feed rectangular patch antennas that can cover BeiDou B1 band (1559.05 – 1563.15 MHz), GPS L1 band (1563 – 1587 MHz), Galileo E1 band (1559 – 1591 MHz), and GLONASS G1 band (1593 – 1610 MHz). The proposed array has a wide frequency bandwidth of 100 MHz (1.55 – 1.65 GHz) with an axial ratio of less than 3 dB. The patch antenna elements are designed on a substrate that has a high dielectric constant to achieve a compact size. The size of each patch element is only $32 \times 32 \times 5.08$ mm^3. These patches are placed along the circumference of a circular aluminium ground plane of 125 mm diameter and 1.5 mm thickness in a 2×2 symmetrical arrangement. The edge-to-edge distance between the opposite patch elements is only 48 mm while for the adjacent elements the separation is only 27 mm. A microwave absorber material is employed to achieve an extremely low mutual coupling level over a wide frequency range (1.55 – 1.65 GHz) within a compact form factor. The proposed design achieves a mutual coupling of less than -20 dB within a compact overall form factor of 125 mm diameter over the entire band of interest. The simulated and measured results of reflection coefficient, mutual coupling, null steering, null depth, and radiation pattern show that the proposed antenna array is an excellent choice for multiband GNSS applications.

INDEX TERMS High isolation, anti-jamming, circularly polarized, wideband antenna.

I. INTRODUCTION

Recently Global Navigation Satellite System (GNSS) anti-jam systems have gained much interest from the research community, which is mainly due to their ability to tackle potential jamming, intentional or unintentional electromagnetic interference and spoofing. Various frequency bands are being used for Radio Navigation Satellite System (RNSS) worldwide. There are two primary Aeronautical Radio Navigation Service (ARNS) bands, which consist of lower L band containing GPS L5, Galileo E5 and GLONASS G3, and upper L band containing GPS L1, BeiDou B1, Galileo E1 and GLONASS G1 [1]. In this paper, our focus is on the GNSS upper L band consisting of GPS L1, BeiDou B1, GLONASS G1 and Galileo E1 bands covering a wide frequency range of 1559 MHz – 1610 MHz.

The compactness of the GNSS antenna array is very critical for portable platforms and mobile terminals. The main challenge in designing a compact GNSS anti-jam antenna array system is the requirement of maintaining a wide impedance bandwidth and at the same time keeping the mutual coupling between different antenna elements to a minimum level.

A number of techniques exist in the literature, that address the issue of mutual coupling in tightly coupled arrays [2]–[6]. But most of these techniques are either narrow band and complex to fabricate or they only address the issue of mutual coupling for linearly polarized antenna arrays. For example, ground plane slots are used in [7] and [8], to decouple patches, monopoles and PIFAs. Similarly, mushroom-shaped Electromagnetic Band Gap structures (EBGs) have been utilized to

reduce the coupling in patch antennas [9], [10]. However, EBGs provide a narrow band isolation and are complex to manufacture if they have vias. Periodic arrangements of ring resonators such as spiral resonators (SRs), split ring resonators (SRRs) and their variants are shown to act as metamaterials with a negative permeability (μ) [11]–[13]. One of the major issues with SRs and SRRs is that they are polarization sensitive and the decoupling performance is dependent upon their alignment with respect to the magnetic field component. Thus, these techniques are shown to work in linearly polarized arrays [11], [12]. However, the GNSS antennas exhibit complex coupling mechanism due to the simultaneous existence of two orthogonal modes for circular polarization (CP) [13]. Some of the works address the mutual coupling for CP antennas such as [13]. However, these are for only GPS L1 or L2 bands and are only suitable for narrowband operation making their utility limited.

In this work, we propose a compact patch antenna array consisting of four identical coaxial-fed square patch elements and a microwave absorber. The designed antenna array covers a wide frequency band of interest (1559 MHz – 1610 MHz) while maintaining an excellent mutual coupling performance (< -20 dB) over the entire spectrum. The proposed antenna array has a compact diameter of only 125 mm. To the best of our knowledge, the proposed antenna array simultaneously covers all the four major GNSS services i.e., GPS, BeiDou, Galileo and GLONASS with the lowest mutual coupling within a compact diameter of only 125 mm (area = 122 cm^2).

The rest of the paper is organized as follows: section II explains the array design procedure, while section III presents some parametric analysis and simulation results. Array fabrication and measured results are presented in section IV. Finally, a conclusion is presented in the last section.

II. DESIGN PROCESS
A. SINGLE ANTENNA ELEMENT
In order to achieve a compact patch antenna element, we have used Rogers TMM10i substrate ($\varepsilon_r = 9.8$, $tan\delta = 0.002$). A standard thickness of 5.08 mm is chosen to cover the entire band of interest (1559 MHz – 1610 MHz). The patch element has a square shape with truncated opposite corners to achieve right hand circular polarization (RHCP) as shown in Fig. 1.
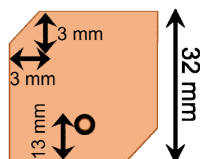

FIGURE 1. Design geometry of single patch antenna element.

GNSS systems use RHCP antennas due to various advantages such as immunity to Faraday Rotation and less multipath propagation losses [14]. For good CP performance, the axial ratio of an antenna should be less than 3 dB [14]. To generate CP in an antenna, the electric field must have

two components that are equal in magnitude and have a phase shift of 90°. There are many techniques to achieve CP such as using dual feed networks, power dividers and phase shifters. However, these techniques increase the design complexity. The simplest approach for generating CP involves exciting the orthogonal modes due to an irregularity in the patch dimensions [14]. Therefore, the opposite corners of the single patch antenna shown in Fig. 1 have been truncated and optimized to achieve a phase shift of 90° with an axial ratio of less than 3 dB. Fig. 2 shows its simulated impedance response and the axial ratio.
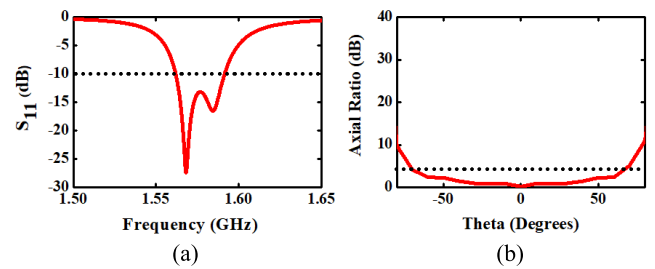

FIGURE 2. Simulation results of single patch antenna. (a) Impedance response. (b) Axial ratio.

B. FOUR ELEMENT ARRAY DESIGN
In contrast to the designs where individual elements are placed in similar orientations [15], we have used the sequentially rotated architecture for our 4-element antenna array. This geometry has been used to generate circular polarization with linearly polarized antenna elements [16]. As thick substrates are known to produce surface waves, therefore we have cut the extra substrate right at the boundary of the metallic patch elements and used an aluminium plate (1.5 mm thick) as a ground plane as shown in Fig. 3. This also gives
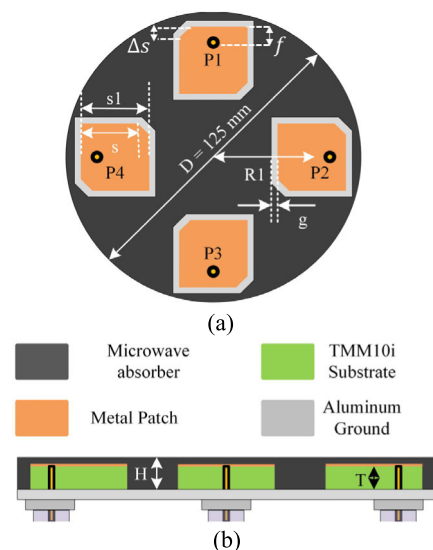

FIGURE 3. The geometry of proposed 4-element patch antenna array for GNSS applications. (a) Top view. (b) Side view.

us an additional benefit of reduced cost as the amount of substrate being consumed is minimized.

Since maximum mutual coupling occurs in E-field coupled antenna elements, thus by using this sequentially rotated architecture the adjacent elements are rotated by 90 degrees. As the antenna elements are sequentially rotated, in order to achieve RHCP gain pattern without any nulls, the ports are fed by $P_1 = 0°$, $P_2 = 90°$, $P_3 = 180°$, and $P_4 = 270°$ phases. As a result of cutting the thick substrate right at the corners of radiating patch elements and placing them in a sequentially rotated array the maximum mutual coupling is reduced to -16 dB for the opposite elements and -14 dB for the adjacent elements. Furthermore, this particular arrangement makes the design perfectly symmetric around the center of the circular ground plane and the placement of two elements on each of the axis allows us to form $N - 1$ nulls, where N is the number of antenna elements [17]. These nulls in the radiation pattern of the array can be independently steered towards the potential sources of EM interference and jamming.

In order to further reduce the mutual coupling, we propose to incorporate a MT-30 microwave absorber ($\varepsilon_r = 15.79$, $tan\delta = 1.944$) in our design. Similar types of absorbers have been used for mutual coupling suppression as in [18] Eccosorb AN-79 has been used for isolation in full-duplex wireless communication systems. However, MT-30 absorber is lighter in weight and less expensive as compared to Eccosorb AN-79. It is filled in between the empty spaces created by cutting the TMM10i substrate (Fig. 3). The introduction of MT-30 in close proximity to the radiating patch elements alters the input impedance of the patches and thus impacts their performance in terms of impedance matching, maximum achievable gain, and axial ratio. Thus, we have re-optimized the locations of feed points for our proposed array and the distance between the edges of the patch elements from the absorber.

III. PARAMETRIC ANALYSIS AND SIMULATED RESULTS

In addition to the location of the feed point, the thickness of the microwave absorber (H), the clearance between the patch elements and the absorber (g), the inter-element distance, which is directly controlled by the distance between the origin of circular ground plate, and the center of each patch ($R1$) are critical design parameters (Fig. 3). For a fixed $R1$, increasing the thickness (H) results in shifting the S_{11} slightly towards lower frequency spectrum and it also widens the impedance matching as shown in Fig. 4.

The gain and mutual coupling tend to decrease with increase in H, this impact is more prominent when H is larger than T, as depicted in Fig. 5.

Increasing the gap g results in an increased gain and mutual coupling, as shown in Fig. 6.

Similarly, the axial ratio tends to get wider with increasing H, and it becomes narrow with increase in g as shown in Fig. 7.
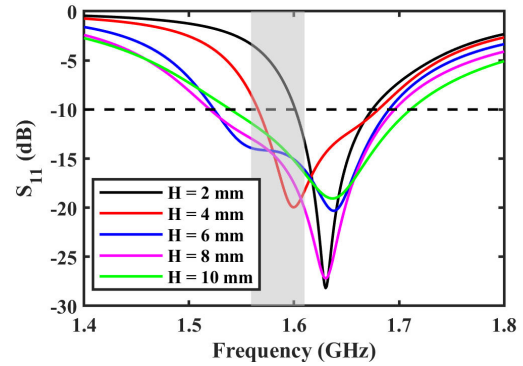

FIGURE 4. Impact of microwave absorber height (H) on impedance matching.
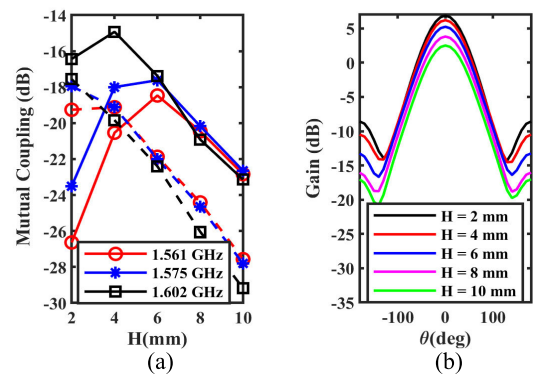

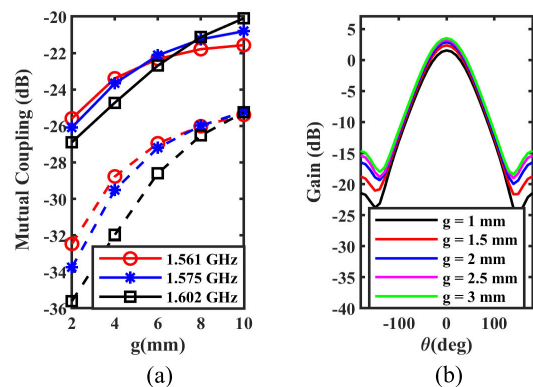**FIGURE 5.** Impact of microwave absorber height (H) on impedance matching.

FIGURE 6. Impact of microwave absorber gap g. (a) On mutual coupling (solid line for adjacent elements S_{12}, and dashed line for opposite elements S_{13}). (b) On array gain.

Thus, there exists a trade-off between mutual coupling, gain and axial ratio. If we want to decrease the mutual coupling and widen the axial ratio (AR) response, we must increase H and decrease g. But it will result in decreased overall gain of the antenna array. It is clear from the above discussion that in order to achieve an optimum performance in which the mutual coupling is less than -20 dB while
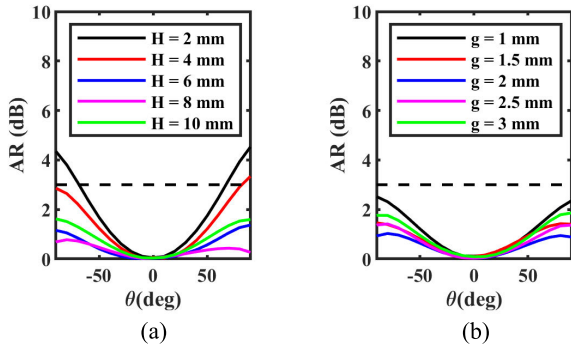
FIGURE 7. Axial ratio variation. (a) With microwave absorber height H. (b) With microwave absorber gap g.

FIGURE 8. Null steering performance of the proposed 4-element wideband GNSS anti-jamming antenna array. (a) Null at −30°. (b) Null at 60°.

keeping the gain performance acceptable we must choose H between 8–10 mm and g between 1.5–2.5 mm. The standard thickness of the commercially available MT-30 microwave absorber is $3.175x$, where x is an integer ranging 1 to 4. In our proposed design, we have chosen $x = 3$ (i.e., $H = 9.525$ mm) while the value of g is chosen to be 1.5 mm so that the array gain is more than 3 dB as shown in Fig. 6(b). The optimized design parameters of our proposed 4-element antenna array are tabulated in Table 1.

TABLE 1. Optimized design parameters.

Parameter	Value (mm)	Parameter	Value (mm)
H	9.525	T	5.08
g	1.5	$R1$	20
$s1$	32	$\varDelta s$	6.6
s	25.4	f	5.7

The null steering performance of the proposed 4-element GNSS anti-jam antenna array is presented in the form of normalized RHCP gain. We have simulated the performance of our proposed wideband GNSS anti-jam antenna array in different jamming scenarios by employing the phase only nulling technique to create nulls in the direction of potential jammers. In the first scenario, we assume a jammer is located at $(\theta = −30°, \Phi = 0°)$ and in the second scenario we assume a jammer is located at $(\theta = 60°, \Phi = 90°)$. The null for first scenario is achieved by turning off ports 2 and 4 and applying a phase shift of 60° between elements 1 and 3 while for the second case the null is generated by turning off ports 1 and 3 and applying a phase shift of 120° between elements 2 and 4. We are steering the null at two different positions i.e., −30° and 60° to assess the anti-jamming performance of our proposed 4-element antenna array. The null depth achieved for the first case is 18 dB while for the second case it is 20 dB. The simulated radiation patterns for both these cases are presented in Fig. 8.
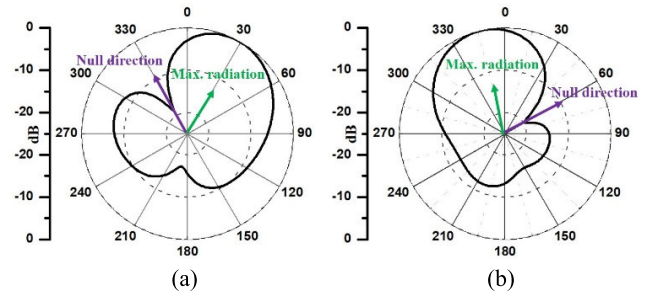
IV. ARRAY FABRICATION AND MEASURED RESULTS

The patch antenna elements are fabricated using LPKF rapid prototype milling machine S103 as shown in Fig. 9. The microwave absorber (MT-30) is a foam-like material which is cut using the same LPKF machine to achieve high accuracy and precision. The aluminium plate is fabricated by using CNC machining and then patch elements are integrated to this plate with the help of a soldering paste. Screws are incorporated to hold the microwave absorber in its position.
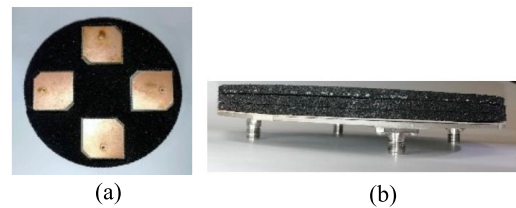

FIGURE 9. Fabricated prototype of the proposed 4-element wideband GNSS anti-jamming antenna array. (a) Top view. (b) Side view.

The fabricated model was then enclosed by using a teflon radome lid to assemble a complete packaged prototype for testing and measurements as shown in Fig. 10.
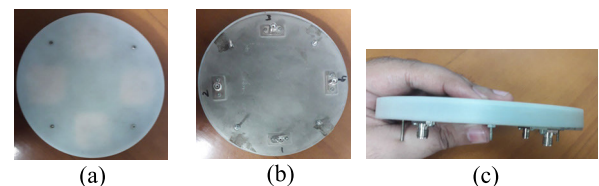

FIGURE 10. Complete assembled prototype of the proposed 4-element wideband GNSS anti-jamming antenna array. (a) Top view. (b) Bottom view. (c) Side view.

The measured impedance matching response is shown in Fig. 11, which depicts an excellent match with the simulations. Since there is a perfect rotational and axial symmetry in the proposed design, therefore, the simulations of reflection coefficient are identical for all four patch elements and can represented by $S_{ii} \forall i \varepsilon \{1, 2, 3, 4\}$.

Similarly, the mutual coupling response S_{ij} can be divided into two categories, i.e., coupling between adjacent

TABLE 2. Performance comparison of our design with related work.

| Ref #	No. of GNSS bands covered	Isolation (dB)	Operating frequency (GHz)	No. of antenna elements	Total Array Area (cm²)	Coupling Reduction Approach	Design Complexity
[13]	L1, L2	> 15, 25	1.227, 1.575	4	119.29	Metamaterial SRR	high
[15]	L1	> 17	1.575	5	254.34	Spatial spacing	low
[19]	L1	> 18.6	1.575	3	153.20	Parasitic strips, Defected Ground Structure	moderate
[20]	L1, L2	> 16, 18	1.205 – 1.240, 1.565 – 1.595	5	400	Artificial Magnetic Conductor	high
[21]	L1, B1	> 20	1.56 – 1.59	4	400	None	high
[22]	L1,B1	> 8-13	1.563 – 1.587	4	138	None	moderate
This Work	**L1, B1, E1, G1**	**> 20**	**1.55 – 1.65**	**4**	**122.65**	**Discontinuous substrate and absorber material**	**low**
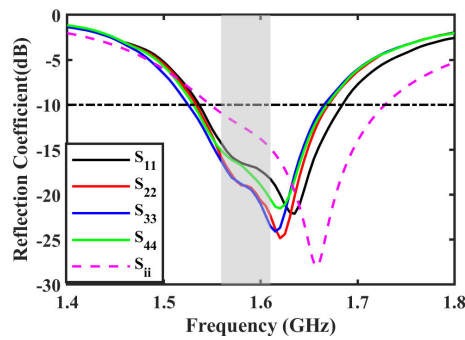
FIGURE 11. Simulated and measured impedance matching performance of proposed 4-element GNSS anti-jam antenna array (solid lines for measured and dashed line for simulated).
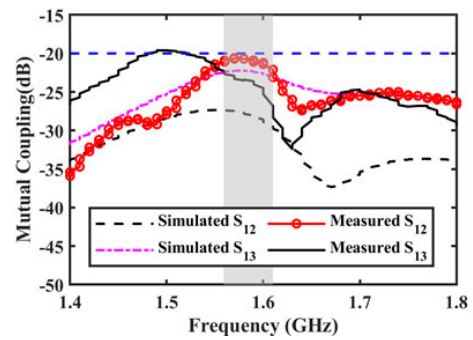

FIGURE 12. Simulated and measured inter-element coupling of proposed 4-element GNSS anti-jam antenna array.

patch elements (S_{12}) and coupling between opposite patch elements (S_{13}). The measured mutual coupling response is shown in Fig. 12. It can be seen that the coupling between opposite patch elements is less than the coupling between adjacent patch elements and each of them is below −20 dB in the entire BW of interest (1559 MHz – 1610 MHz). To the best of author's knowledge this is the minimum reported mutual coupling that incorporates all the four major GNSS bands within a compact diameter of 125 mm.

The radiation pattern of the proposed array was also measured in the anechoic chamber for all the frequency bands. Fig. 13 shows the simulated and measured *E-plane* and *H-plane* normalized radiation pattern for the GPS L1 band i.e., 1.575 GHz for a single antenna element of our proposed array.

If all the elements of the array are excited with a phase shift of 0° at each port, then a null is formed at the boresight. The measured null depth is more than 30 dB in this case as shown in Fig. 14.
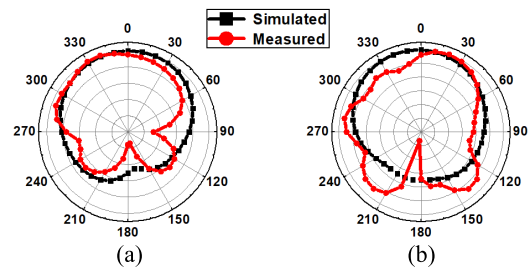

FIGURE 13. Normalized simulated and measured radiation pattern for 1.575 GHz. (a) E-plane. (b) H-plane.

Fig. 15 shows our proposed antenna array placed in the anechoic chamber for radiation pattern measurement.

Table 2 shows the comparison of our proposed wideband anti-jamming antenna array with other published literature. As compared to the earlier reported works that cover either one or two GNSS bands [8], [9], [13]–[16], our proposed antenna array simultaneously covers all the four major GNSS bands with a bandwidth of more than 100 MHz
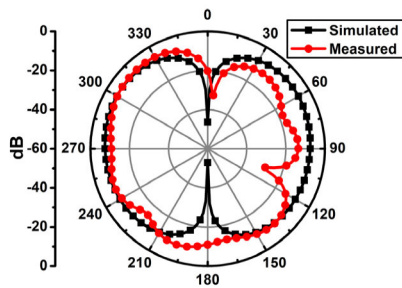
FIGURE 14. Simulated and measured radiation pattern with a null at boresight.
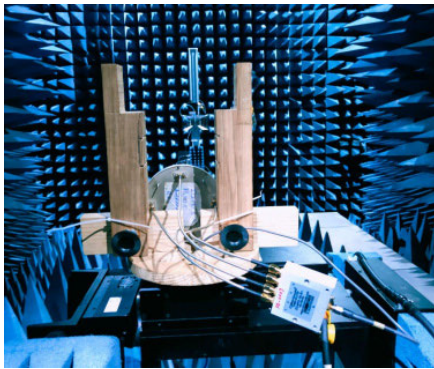

FIGURE 15. Radiation pattern measurement setup for the proposed antenna array.

(1.55 – 1.65 GHz). Furthermore, our design has the least mutual coupling (< -20 dB) within a compact area of only 122 cm^2 (125 mm diameter) as compared to other designs that have a significantly larger size. As compared to other isolation techniques such as EBGs and SRRs that require more substrate and costly fabrication, our proposed design incorporates an aluminum ground plane to reduce the cost of substrate being used and employs a low-cost microwave absorber to achieve a wideband isolation level.

V. CONCLUSION

This work presents a compact 4-element GNSS antenna array design that achieves a mutual coupling level of less than -20 dB within a highly compact form factor of only 125 mm. The design uses a low-cost approach in which four identical antenna elements of 32×32 mm^2 are cut and placed on an aluminium ground plane to reduce the coupling due to the surface waves along with a microwave absorber material to further minimize the coupling that exists due to space wave propagation as well. The proposed design exhibits excellent null steering performance with null depths of more than 18 and 20 dB over a wide range of scanning angles in the upper hemisphere. The array covers a wide frequency spectrum from 1.55 to 1.65 GHz with an isolation level of more than 20 dB in this entire bandwidth. The axial ratio of the designed array is less than 3 dB for good CP performance.

The proposed design achieves the lowest level of mutual coupling reported so far for a wideband GNSS patch antenna array within a compact area of only 122 cm^2, that can cover the entire bandwidth of interest (1559 MHz – 1610 MHz). The proposed design is suitable for applications that require simultaneous operation in all the four major bands of the GNSS upper L band i.e., GPS L1, BeiDou B1, Galileo E1 and GLONASS G1.

REFERENCES

[1] *GNSS Signal-Navipedia*. Accessed: Sep. 9, 2021. [Online]. Available: https://gssc.esa.int/navipedia/index.php/GNSS_signal

[2] A. A. Althuwayb, "Low-interacted multiple antenna systems based on metasurface-inspired isolation approach for MIMO applications," *Arabian J. Sci. Eng.*, pp. 1–10, May 2021.

[3] M. Alibakhshikenari, M. Khalily, B. S. Virdee, C. H. See, R. Abd-Alhameed, and E. Limiti, "Mutual coupling suppression between two closely placed microstrip patches using EM-bandgap metamaterial fractal loading," *IEEE Access*, vol. 7, pp. 23606–23614, 2019.

[4] M. Alibakhshikenari, M. Khalily, B. S. Virdee, C. H. See, R. A. Abd-Alhameed, and E. Limiti, "Mutual-coupling isolation using embedded metamaterial EM bandgap decoupling slab for densely packed array antennas," *IEEE Access*, vol. 7, pp. 51827–51840, 2019.

[5] M. Alibakhshikenari, F. Babaeian, B. S. Virdee, S. Aïssa, L. Azpilicueta, C. H. See, A. A. Althuwayb, I. Huynen, R. A. Abd-Alhameed, F. Falcone, and E. Limiti, "A comprehensive survey on 'various decoupling mechanisms with focus on metamaterial and metasurface principles applicable to SAR and MIMO antenna systems'," *IEEE Access*, vol. 8, pp. 192965–193004, 2020.

[6] M. Alibakhshikenari, B. S. Virdee, L. Azpilicueta, M. Naser-Moghadasi, M. O. Akinsolu, C. H. See, and B. Liu, "A comprehensive survey of 'metamaterial transmission-line based antennas: Design, challenges, and applications'," *IEEE Access*, vol. 8, pp. 144778–144808, 2020.

[7] C.-Y. Chiu, C.-H. Cheng, R. D. Murch, and C. R. Rowell, "Reduction of mutual coupling between closely-packed antenna elements," *IEEE Trans. Antennas Propag.*, vol. 55, no. 6, pp. 1732–1738, Jun. 2007.

[8] M. M. B. Suwailam, O. F. Siddiqui, and O. M. Ramahi, "Mutual coupling reduction between microstrip patch antennas using slotted-complementary split-ring resonators," *IEEE Antennas Wireless Propag. Lett.*, vol. 9, pp. 876–878, 2010.

[9] F. Yang and Y. Rahmat-Samii, "Microstrip antennas integrated with electromagnetic band-gap (EBG) structures: A low mutual coupling design for array applications," *IEEE Trans. Antennas Propag.*, vol. 51, no. 10, pp. 2936–2946, Oct. 2003.

[10] E. Rajo-Iglesias, Ó. Quevedo-Teruel, and L. Inclan-Sanchez, "Mutual coupling reduction in patch antenna arrays by using a planar EBG structure and a multilayer dielectric substrate," *IEEE Trans. Antennas Propag.*, vol. 56, no. 6, pp. 1648–1655, Jun. 2008.

[11] K. Buell, H. Mosallaei, and K. Sarabandi, "Metamaterial insulator enabled superdirective array," *IEEE Trans. Antennas Propag.*, vol. 55, no. 4, pp. 1074–1085, Apr. 2007.

[12] M. M. Bait-Suwailam, M. S. Boybay, and O. M. Ramahi, "Electromagnetic coupling reduction in high-profile monopole antennas using single-negative magnetic metamaterials for MIMO applications," *IEEE Trans. Antennas Propag.*, vol. 58, no. 9, pp. 2894–2902, Sep. 2010.

[13] A. A. Gheethan, P. A. Herzig, and G. Mumcu, "Compact 2×2 coupled double loop GPS antenna array loaded with broadside coupled split ring resonators," *IEEE Trans. Antennas Propag.*, vol. 61, no. 6, pp. 3000–3008, Jun. 2013.

[14] A. Z. Narbudowicz, "Advanced circularly polarised microstrip patch antennas," Ph.D. dissertation, Dublin Inst. Technol., Dublin, Ireland, 2013.

[15] K. Wu, L. Zhang, Z. Shen, and B. Zheng, "An anti-jamming 5-element GPS antenna array using phase-only nulling," in *Proc. 6th Int. Conf. ITS Telecommun.*, Jun. 2006, pp. 370–373.

[16] J. Huang, "A technique for an array to generate circular polarization with linearly polarized elements," *IEEE Trans. Antennas Propag.*, vol. AP-34, no. 9, pp. 1113–1124, Sep. 1986.

[17] W. Kunysz, "Advanced pinwheel compact controlled reception pattern antenna (AP-CRPA) designed for interference and multipath mitigation," in *Proc. 14th Int. Tech. Meeting Satell. Division Inst. Navigat.*, Salt lake City, UT, USA, Sep. 2001, pp. 2020–2036.

[18] E. Everett, A. Sahai, and A. Sabharwal, "Passive self-interference suppression for full-duplex infrastructure nodes," *IEEE Trans. Wireless Commun.*, vol. 13, no. 2, pp. 680–694, Jan. 2014.

[19] G. Byun, H. Choo, and S. Kim, "Design of a small arc-shaped antenna array with high isolation for applications of controlled reception pattern antennas," *IEEE Trans. Antennas Propag.*, vol. 64, no. 4, pp. 1542–1546, Apr. 2016.

[20] S. X. Ta and I. Park, "A single-feed dual-band antenna for an anti-jam GPS array," in *Proc. Int. Workshop Antenna Technol. (iWAT)*, Mar. 2015, pp. 327–329.

[21] Y. Liu, S. Zhang, and Y. Gao, "A high-temperature stable antenna array for the satellite navigation system," *IEEE Antennas Wireless Propag. Lett.*, vol. 16, pp. 1397–1400, 2017.

[22] B. R. Rao, J. H. Williams, C. D. Boschen, J. T. Ross, E. N. Rosario, and R. J. Davis, "Characterizing the effects of mutual coupling on the performance of a miniaturized GPS adaptive antenna array," in *Proc. 13th Int. Tech. Meeting Satell. Division Inst. Navigat.*, Salt lake City, UT, USA, Sep. 2000, pp. 2491–2498.

ABDULLAH MADNI received the B.S. degree in electronic engineering from the Ghulam Ishaq Khan Institute of Engineering Sciences and Technology (GIKI), Pakistan, in 2015, and the M.S. degree in electrical engineering from the Information Technology University (ITU), Punjab, Pakistan, in 2018. He is currently pursuing the Ph.D. degree in electrical engineering with the Lahore University of Management Sciences (LUMS), Pakistan. His main research interests include design of wideband antenna arrays for satellite communication, isolation enhancement in antenna arrays, and designing antennas for 5G systems.

MUHAMMAD AWAIS received the B.S. degree in electrical engineering from the COMSATS Institute of Information Technology (CIIT), Pakistan, in 2013, and the M.S. degree in electrical engineering from the Lahore University of Management Sciences (LUMS), Pakistan, in 2018. He is currently pursuing the Ph.D. degree in electrical engineering with The University of Texas at Dallas. His research interests include the design of ultra-wideband and mmWave antennas, high-frequency electronic circuits, and reflectarray antennas.

WASIF TANVEER KHAN (Member, IEEE) received the B.Sc. degree in electrical engineering from the University of Engineering and Technology, Lahore, Pakistan, in 2005, and the M.S. and Ph.D. degrees in electrical and computer engineering from the Georgia Institute of Technology, Atlanta, USA, in 2010 and 2014, respectively.

From January 2006 to December 2008, he was a Lecturer with the National University of Computer and Emerging Sciences-FAST, Lahore. Dr. Khan was awarded the M.S. Leading to Ph.D. Fulbright Scholarship in 2008. Since January 2015, he has been working as an Assistant Professor with the Department of Electrical Engineering, Lahore University of Managements Sciences (LUMS), Pakistan. He has authored/coauthored more than 60 research papers in peer-reviewed conferences and journals.

• • •